Geomagnetic Secular Variations at the Permian-Triassic Boundary and Pulsed Magmatism During Eruption of the Siberian Traps

Vladimir E. Pavlov, Frederic Fluteau, Anton V. Latyshev, Anna M. Fetisova, Linda T. Elkins-Tanton, Ben A. Black, Seth D. Burgess, Roman V. Veselovskiy

Geochemistry, Geophysics, Geosystems

AGU100 ADVANCING EARTH AND SPACE SCIENCE

RESEARCH ARTICLE
10.1029/2018GC007950

Key Points:
- Siberian Traps were formed during a limited number of volcanic pulses
- The 3.5 km of lavas in Northern Siberia was erupted during ~10,000 years
- Secular variations ~250 Ma were about the same as during the latest Cenozoic

Supporting Information:
- Supporting Information S1
- Table S1

Correspondence to:
R. V. Veselovskiy,
roman.veselovskiy@ya.ru

Citation:
Pavlov, V. E., Fluteau, F., Latyshev, A. V., Fetisova, A. M., Elkins-Tanton, L. T., Black, B. A., et al. (2019). Geomagnetic secular variations at the Permian-Triassic boundary and pulsed magmatism during eruption of the Siberian Traps. *Geochemistry, Geophysics, Geosystems*, *20*, 773–791. https://doi.org/10.1029/2018GC007950

Received 10 SEP 2018
Accepted 14 JAN 2019
Accepted article online 17 JAN 2019
Published online 5 FEB 2019

Geomagnetic Secular Variations at the Permian-Triassic Boundary and Pulsed Magmatism During Eruption of the Siberian Traps

Vladimir E. Pavlov[1,2], Frederic Fluteau[3], Anton V. Latyshev[1,4], Anna M. Fetisova[1,4], Linda T. Elkins-Tanton[5], Ben A. Black[6], Seth D. Burgess[7], and Roman V. Veselovskiy[1,4]

[1]Schmidt Institute of Physics of the Earth, Russian Academy of Sciences, Moscow, Russia, [2]Institute of Geology and Petroleum Technologies, Kazan (Volga region) Federal University, Kazan, Russia, [3]Institut de Physique du Globe de Paris, Paris Diderot University, Paris, France, [4]Geological Department, Lomonosov Moscow State University, Moscow, Russia, [5]School of Earth and Space Exploration, Arizona State University, Tempe, AZ, USA, [6]Department of Earth and Atmospheric Sciences, The City College of New York, New York, NY, USA, [7]Volcano Science Center, U.S. Geological Survey, Anchorage, AK, USA

Abstract The tempo of Large Igneous Province emplacement is crucial to determining the environmental consequences of magmatism on the Earth. Based on detailed flow-by-flow paleomagnetic data from the most representative Permian-Triassic Siberian Traps lava stratigraphy of the northern Siberian platform, we present new constraints on the rate and duration of the volcanic activity in the Norilsk and Maymecha-Kotuy regions. Our data indicate that volcanic activity there occurred during a limited number of short volcanic pulses, each consisting of multiple individual eruptions, and that the total duration of discrete eruption pulses did not exceed ~10,000 years (hiatuses are not included). Our study confirms the occurrence of a thick interval in the lower part of the Norilsk lava sections, which contains a record of geomagnetic reversal and excursion. Based on combined evidence from paleomagnetic secular variation and typical timescales for such reversals, we conclude that the ~1-km-thick lava stratigraphy, corresponding to ~20,000 km^3 of basalt, of the Kharaelakh, Norilsk, and Imangda troughs was formed during a brief, but voluminous, eruptive period of several thousand years or less. Our data further suggest that the ore-bearing Norilsk-type intrusions are coeval or nearly coeval with the boundary between the Morongovsky and Mokulaevsky formations. We calculated a new Siberian Permian-Triassic paleomagnetic pole Norilsk-Maymecha-Kotuy (NMK): PLat = 52.9°, PLong = 147.1°, A95 = 4.3°, K = 23.2, and N = 49 lava flows. It is shown that geomagnetic field variations circa 252 Ma were similar to those observed in the latest Cenozoic.

1. Introduction

The Siberian Traps represent one of the largest continental igneous provinces on Earth, with a minimum total volume of 2–4 × 10^6 km^3 (Vasil'ev et al., 2000). The source of the Siberian Traps basalt was, probably, a mantle plume, the center of which was located in the southern Taymyr region under the focus of a coupled giant circumferential and radiating dyke swarm system (Buchan & Ernst, 2019). Siberian Traps magmatism was coeval with the Permian-Triassic extinction, which occurred over 60 ± 48 ka between 251.941 ± 0.037 and 251.880 ± 0.031 Ma (Burgess et al., 2014). Geochronological data suggest that most of the volume of the Siberian Traps was erupted over ~300,000 years before the Permian-Triassic extinction, and eruptions continued for at least 500,000 years after the extinction (Burgess et al., 2017; Burgess & Bowring, 2015). The Permian-Triassic extinction is the largest known mass extinction event in the Phanerozoic, with more than 90% of marine species and more than 70% of terrestrial species (including insects) disappeared. The extinction crisis was also accompanied by strong perturbations in seawater chemistry, notably in the carbon cycle record (e.g., C. Korte et al., 2004, for a review). Although in multiple cases geochronology shows that the emplacement of Large Igneous Provinces (LIPs) has coincided with mass extinctions or intervals of environmental stress (Blackburn et al., 2013; Courtillot & Renne, 2003; Kamo et al., 1996, 2003; Reichow et al., 2009; Renne et al., 2015; Schoene et al., 2015), the precise causal relationship between Siberian Traps volcanism and the Permo-Triassic (PT) mass extinction remains controversial.

LIP volcanism can release large amounts of volatiles (carbon dioxide, sulfur, fluorine, and chlorine) that originated both from mantle melting (e.g., Saunders et al., 2015) and from assimilation or contact heating

of country rocks (Black et al., 2012, 2015; Svensen et al., 2009). Volcanic sulfur aerosols from recent explosive eruptions are capable of causing transient changes in global climate (e.g., Robock, 2000). In the case of LIPs, the total quantities of gas released in the climatic system are several orders of magnitude greater than those observed during recent and historical eruptions and, as a consequence, it has been proposed that LIP volcanism is a likely cause of strong environmental perturbations (e.g., Black et al., 2012, 2018; Chenet et al., 2008, 2009; Self et al., 2006; Schmidt et al., 2016; Svensen et al., 2009).

The tempo of volcanism is critical to assessing the effects of volatiles release. Indeed, if the emplacement of the Siberian Traps occurred more or less evenly over a period of ~1 Myr (Burgess & Bowring, 2015; Kamo et al., 1996, 2003; Reichow et al., 2009), it would yield a minimum estimate of mean eruption rate over this interval of about ~3 km^3/year. This rate is roughly similar to global basalt production at modern mid-ocean ridges (3 km^3/year), and lower than that observed during the 1783–1784 Laki eruption, which produced ~15 km^3 of magma in 8 months (Thordarson & Self, 2003). From the time-averaged rate of magma emplacement alone, it is thus challenging to understand the causal links between the Siberian Traps and the PT mass extinction.

Paleomagnetic evidence suggests at least two LIPs—the Deccan Traps (Chenet et al., 2008, 2009) and the Karoo Traps (Moulin et al., 2011, 2017)—were built by a series of brief and voluminous volcanic pulses. In the case of the Deccan Traps, high-precision geochronology suggests these pulses might represent higher-frequency modulations embedded within longer-term variations in magma emplacement rates (e.g., Renne et al., 2015; Richards et al., 2015; Schoene et al., 2015). Here we present new detailed paleomagnetic data obtained from the most representative lava sections of the Siberian Traps, those in the Maymecha-Kotuy and Norilsk regions (Figure 1). These data allow us to develop important duration constraints on volcanic activity in the north part of the Siberian platform close to the PT boundary. Data obtained in this study allowed us to calculate the scatter of virtual geomagnetic poles (VGP scatter), which is commonly accepted to be a measure of the secular variations of the geomagnetic field. Study of changes in geomagnetic secular variations through geological time is essential to document the Earth's magnetic field evolution and provides important data for geodynamo modeling.

2. Geologic Background

The stratigraphic sections examined for this study are in the northern part of the Siberian platform, in the Norilsk region (the Sunduk and Ergalakh sections) and in the Maymecha-Kotuy region (the Medvezhya and Truba sections, Kotuy river valley; Figure 1).

The Norilsk region is in the northwest corner of the main Siberian Traps exposure extent and is the most thoroughly studied region of the Siberian Traps province due to the presence of extensive Cu-Ni-Pt deposits. The volcanic sequence in Norilsk overlies the Permian (Carboniferous-Permian) sedimentary rocks of the Tungusskaya series and includes 11 formations with a total thickness of about 3.5 km (Figure 2). Tholeiitic basalts predominate in the lava stratigraphy; picritic basalts, trachybasalts, and mafic tuffs are present in smaller quantities throughout the stratigraphy. The lowermost Ivakinsky Formation contains subalkaline lavas (trachybasalts) and is considered to be Upper Permian, while the other formations are considered to be Lower Triassic (Fedorenko & Czamanske, 1997). On the other hand, Burgess and Bowring (2015) and Burgess et al. (2017) argue that the lava pile of the Norilsk region was emplaced just before the PT boundary.

The Norilsk-1 intrusion, which is suggested (Lind et al., 1994) to be comagmatic with the volcanic Morongovsky Formation (the middle part of the composed Norilsk section) is dated at 251.1 ± 0.3 Ma by the U-Pb method on zircon and baddeleyite (Kamo et al., 1996) and at 251.907 ± 0.067 Ma by the U-Pb method on zircon (Burgess & Bowring, 2015; Figure 2).

The Maymecha-Kotuy region is in the northeast corner of the Siberian Traps (Figure 1). This region appears to be the only region in the Siberian Traps where alkaline and ultramafic lavas predominate over tholeiitic basalts. The volcanic sequence comprises six formations overlying the Tungusskaya sedimentary series (Figure 2). The total thickness of the lava stratigraphy reaches ~4 km (Fedorenko & Czamanske, 1997). The latest stage of igneous activity in this region occurs in the multiphase Guli intrusion (Kamo et al., 2003), which is composed of alkaline and ultramafic magmas and carbonatites. The Arydzhangsky

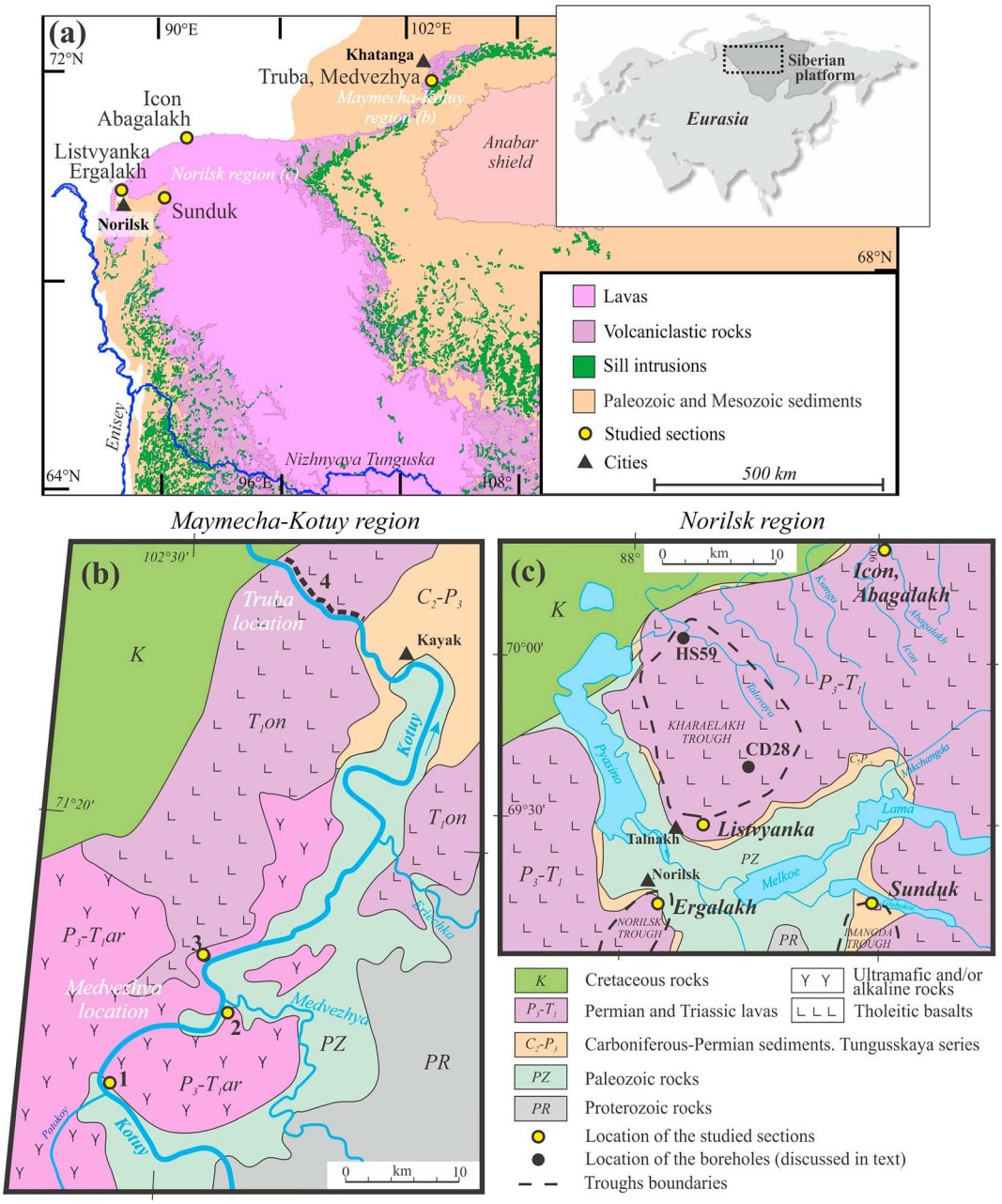

Figure 1. (a) Sketch geological map of the northwestern Siberian platform with location of the studied sections (modified from Svensen et al., 2009). (b) Studied volcanic sections of Maymecha-Kotuy region: 1–3 = Medvezhya; 4 = Truba; ar = Arydzhangsky Formation, kg = Onkuchaksky Formation (Kogotoksky Series). (c) Studied volcanic sections of Norilsk region (CD28 and HS59 are boreholes).

Formation, located in the lower part of the Maymecha-Kotuy section, has been dated at 251.7 ± 0.4 Ma (Kamo et al., 2003) and 252.24 ± 0.12 Ma (Burgess & Bowring, 2015) by U-Pb in perovskite.

The Delkansky Formation, representing the upper part of the volcanic sequence of the region, is dated at 251.1 ± 0.3 (middle part of the Formation; Kamo et al., 2003), 251.901 ± 0.061, and 251.483 ± 0.088 Ma (lower and middle parts, respectively; Burgess & Bowring, 2015) by U-Pb in zircon (Figure 2).

The lava flows of the Norilsk region were sampled at two sections (Figure 1c). First, the Sunduk section (750 m thick) contains the lower half of the Norilsk volcanic sequence from the Ivakinsky to the

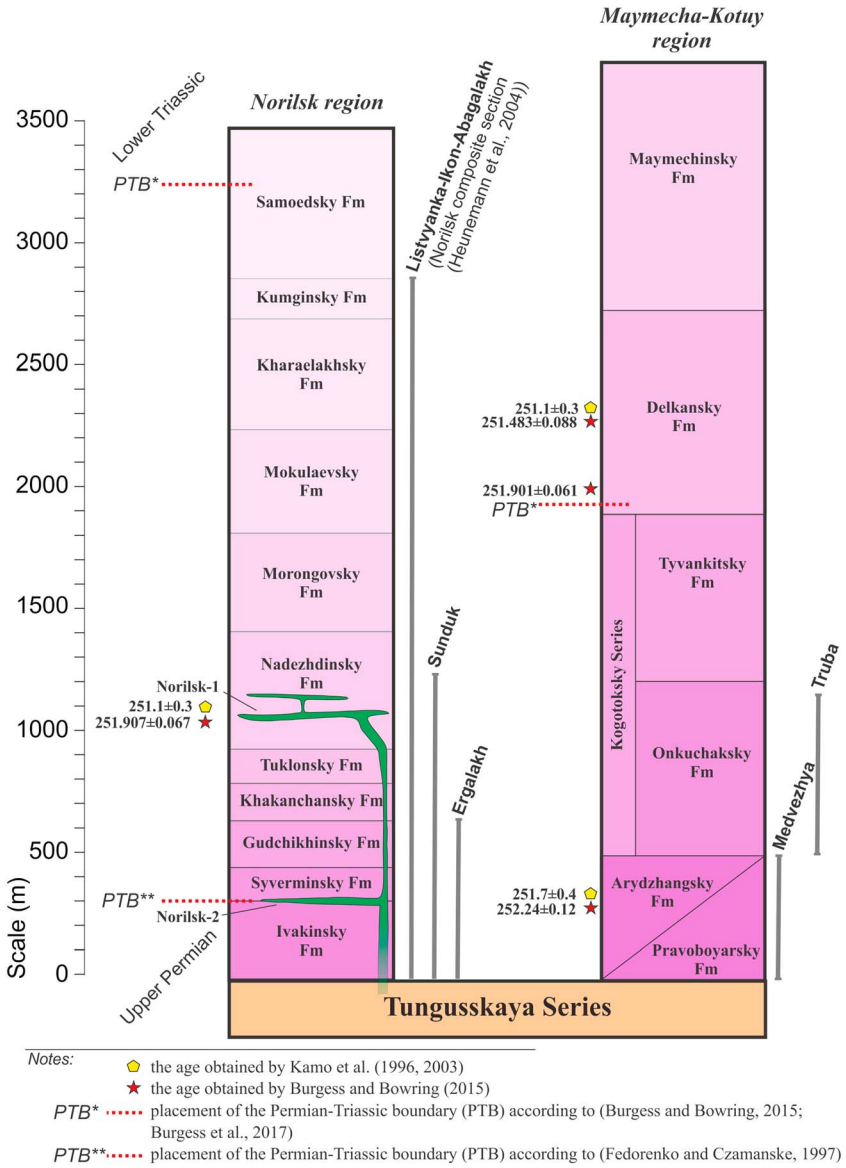

Figure 2. Stratigraphy (modified from Kamo et al., 2003) and isotopic ages (see text for details) of volcanic sequences of Norilsk and Maymecha-Kotuy regions. Stratigraphic positions of discussed sections (gray bars) and intrusions (green) are also shown.

Nadezhdinsky Formation and consists of 42 units of tholeiitic and picritic lavas and mafic tuffs. The second section, the 180-m-thick Ergalakh, corresponds to the lowest part of the Norilsk volcanic sequence. Here we sampled 12 basaltic lava flows of the Ivakinsky, Syverminsky, and Gudchikhinsky Formations. We also sampled the Norilsk-2 intrusion, which cuts the lava pile of the Ergalakh section. This intrusion belongs to the same Norilsk type as intrusion Norilsk-1 and is considered to be coeval to it (Naldrett, 2003).

Volcanic rocks of the Maymecha-Kotuy region were sampled at two sections (Figure 1b) located along the Kotuy River valley: near the mouth of its tributary, the Medvezhya River (Medvezhya section, 250 m thick), and near the Kayak settlement (Truba section, 350 m thick). These lava sections, in total about 600 m thick, present the most complete volcanic sequence in the Kotuy River basin and, taken together, hereinafter are referred to as composite Kotuy section.

The Medvezhya section (Fedorenko et al., 2000; sections 4 and 1) contains 37 units (mostly lavas) of the Arydzhangsky Formation, which consists of melanephelinite, augitite, and other alkaline-ultramafic rocks interlayered in the lower part of the section with alkaline-ultramafic tuffs. The Truba section contains 42 tholeiitic flows of the Onkuchaksky Formation along with one thick (30 m) unit of basaltic tuffs in the lower part of the section.

All the studied rocks are flat-lying except in the Truba section, where flows have a slight dip to the northwest of 3–5°. Since the sedimentary rocks of the nearby Tungusskaya sedimentary series lie flat, we suggest that the dip of the Truba flows represents original local paleotopography.

3. Methods

The analysis of geomagnetic paleosecular variations recorded by lava flows provides valuable information on the tempo of volcanic activity. During cooling, volcanic flows acquire thermoremanent magnetization that records the direction of the geomagnetic field at the site and time of the emplacement. The direction of the geomagnetic field changes rather quickly on geological timescales. Based on the data obtained by Gallet et al. (2002) for geomagnetic secular variations in Europe for the last 3,000 years, Chenet et al. (2008) calculated the distribution of SV velocities along tracks, which describe the evolution of declination and inclination during this time period. They have found that this distribution has lognormal shape with a strong mode at about 2° per century.

If we assume this value as a mean secular variation rate, then given that the accuracy of measurement of paleomagnetic direction in lava flows is 4° to 8°, flows that erupted more than 300–400 years apart should have statistically different paleomagnetic directions. On the other hand, lava flows that form within 300–400 years of each other would have statistically indistinguishable paleomagnetic directions.

Therefore, if the mean directions of neighboring flows do not differ statistically (e.g., at the 95% confidence level) we can unite them into a single directional group (DG), corresponding to a volcanic pulse. Hereinafter we will use the term “volcanic pulse” to designate short bursts of volcanic activity that are separated from other volcanic pulses by relatively longer periods of quiescence; each volcanic pulse corresponds to two or more lava flows.

Different methods have been employed to determine groups of statistically similar magnetic directions. Mankinen et al. (1985) and Jarboe et al. (2008) used two criteria that must be satisfied to define a DG: the mean magnetic directions of the N flows composing the DG must not show a clear trend and their cones of confidence α_{95} must overlap. P. Riisager et al. (2002, 2003) used the test of Watson (1956), which consists in calculating the statistic F based on R values and compare the result with a tabulated F value for the degree of freedom. Knight et al. (2004) combined two criteria: “the variation of the directional group is less than the A95 of the mean group direction and the jump in the direction is greater than the mean A95 of the previous group”. Chenet et al. (2008) defined a DG based on whether the distances between the mean magnetic direction of the DG and each site-mean direction of lava flows supposed to belong to the DG are less than a threshold defined as the square root of the sum of the squares of the 95% confidence cones of the DG and respective paleomagnetic sites. Site-mean directions with confidence values α_{95} in excess of 10° were excluded.

In this work, we followed the procedure as proposed by Chenet et al. (2008, 2009), and also used by Moulin et al. (2011, 2017). The number of DGs and individual directions (IDs, corresponding to individual flows, which mean paleomagnetic directions are statistically different from these ones of adjacent flows) corresponds to the number of volcanic pulses and individual eruptions that formed the studied section.

Following Chenet et al. (2008, 2009), the total time of emplacement of flows due to volcanic pulses or individual eruptions could correspond to a time interval as short as 100 years. However, in distinction from Chenet et al. (2008, 2009), we assume the somewhat more conservative estimate of 300 to 400 years' duration for producing a volcanic pulse consisting of more than one flow, to be consistent with the statistical 95% confidence interval of our measurement technique. In fact, the secular variation rate may be much faster than 2° per century (see, e.g., the British archeomagnetic master curve, presented by Batt et al., 2017). In this case, our estimation of pulse duration may be considered as a maximum.

The angular dispersion of virtual geomagnetic poles (VGP scatter) (here denoted S_B) is generally accepted as a measure of the paleosecular variations. Similar to Biggin et al. (2008), in our study we calculated S_B as follows:

$$S_B = \left[\frac{1}{N-1}\sum_{i=1}^{N}\left(\Delta_i^2 - \frac{S_{w_i}^2}{\mathrm{n}_i}\right)\right]^{1/2} \qquad (i = 1, ..., N)$$

where Δi gives the angular distance of the ith VGP, calculated each for ith flow, from the mean VGP. S_{Wi} is the within-site dispersion of VGPs calculated for each sample within ith flow. N is the number of flows, n_i is the number of samples taken from ith flow, and

$$S_{w_i}^2 = 81\sqrt{K},$$

where (according to Cox, 1970)

$$\mathrm{K} = k\left(\frac{1}{8}\left(5 + 18\sin^2\lambda + 9\sin^4\lambda\right)\right)^{-1},$$

k is a Fisherian precision parameter for directions within sites, and λ is the paleolatitude of the site.

A cutoff angle is commonly used to exclude the outliers produced by measurements or by records and to focus on the geomagnetic field variations beyond the reversals and excursions. In our study we calculate this cutoff angle following the iterative procedure described by Vandamme (1994). However, to ensure that our results can be compared with results from other studies, we also report the Sb value obtained when applying fixed 45° cutoff angle (e.g., Johnson et al., 2008).

Volcanic pulses can be represented by different amount of volcanic flows. In this case, if we use VGPs obtained from every flow, the final estimate can be biased. To avoid this we use mean DG directions rather than mean directions obtained from individual flows for calculation of the VGPs dispersion.

Between 8 and 20 independent samples were taken from each lava flow or tuff unit in the studied sections. Hand samples were oriented using a magnetic compass with a control for possible deflection of the compass needle due to the strongly magnetized rocks. In total about 1,400 samples were taken from the Norilsk and Maymecha-Kotuy regions.

In addition to our own data, we included in our interpretation the paleomagnetic results of Heunemann et al. (2004) from the Listvjanka, Icon, Abagalakh, and Talnakh sections in the Norilsk area (Figure 1).

4. Magnetic Mineralogy

Investigations of the magnetic mineralogy as well as demagnetization procedures were undertaken at the Institute of Physics of the Earth (Moscow, Russia). Thermomagnetic curves of the saturation magnetization, measured in the field around 800 mT, were used to identify the magnetic minerals, the carriers of magnetization. Additionally, we carried out measurements of the temperature variations of magnetic susceptibility. Electron microscopy and microprobe analyses were used to determine the structure and composition of magnetic minerals.

Our samples from the Arydzhangsky Formation (Figures 3a and 3b) contain a magnetic phase with a Curie point between 540 and 590 °C. SEM images and microprobe analyses show that this phase is probably relatively low-titanium titanomagnetite and/or magnetite. Occurrence of exsolution lamellae is a clear indication of high-temperature (HT) oxidation of titanomagnetite, and is evidence for a primary origin of magnetic minerals.

Occasionally, a second phase with a Curie point around 450 °C and, possibly, a third one with a Curie point around 300 °C is observed in the susceptibility versus temperature curves. These may reflect some quantity of primary unexsolved titanomagnetite grains.

Electron microscope and microprobe analyses reveal the occurrence of extensively altered, exsolved titanomagnetite grains with relicts of magnetite and ilmenite lamellae. In several samples we found secondary

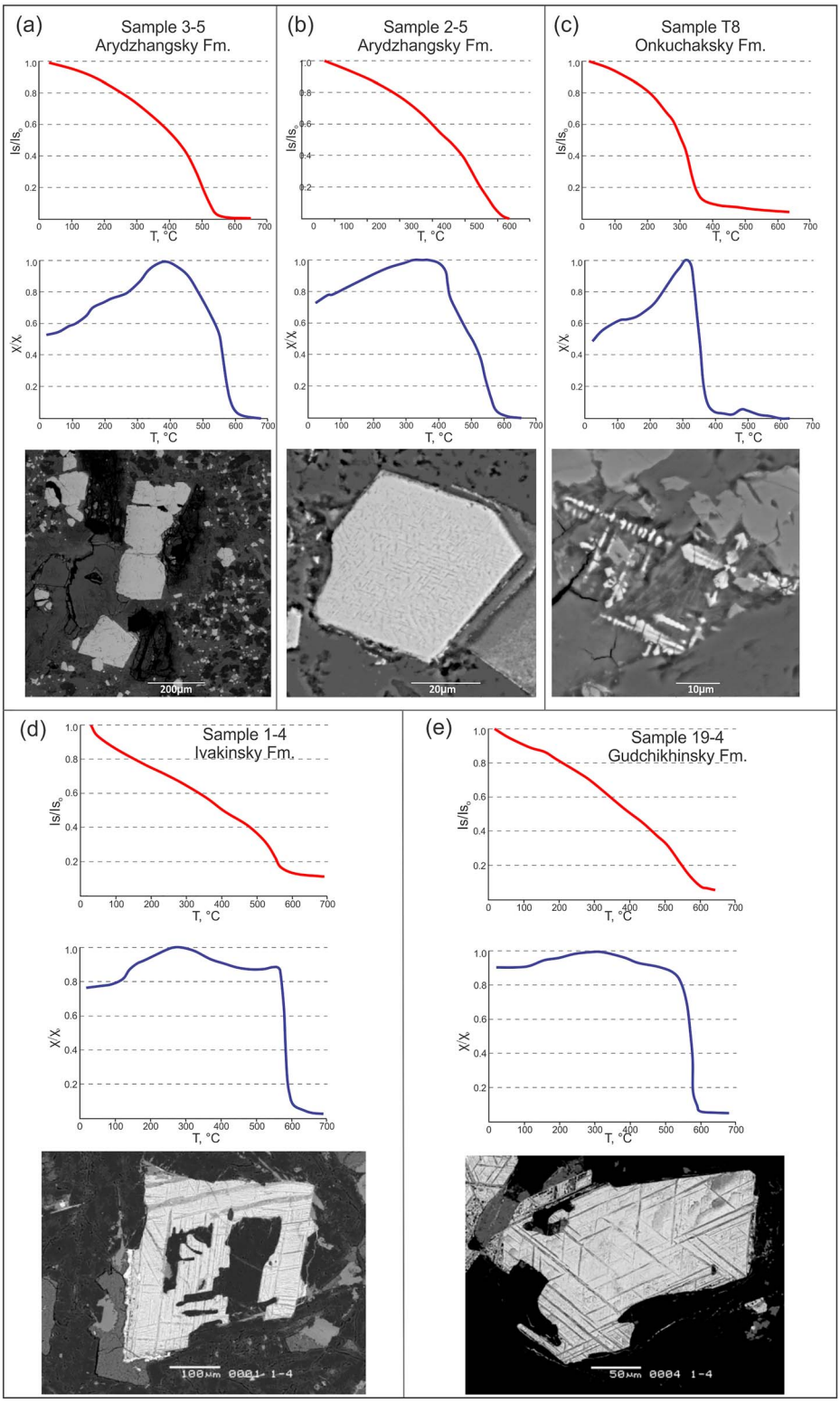

Figure 3. Magnetic mineralogy of the studied rock from the Kotuy (a–c) and Norilsk (d and e) regions. Thermomagnetic curves and SEM images of (a) primary magmatic titanomagnetite and (b) exsolved titanomagnetite grains, Arydzhangsky Formation; (c) primary titanomagnetite grains with dendritic and cruciform quench structure, Onkuchaksky Formation; (d) exsolved grains of titanomagnetites, Ivakinsky Formation, and (e) exsolved grains of titanomagnetites, Gudchikhinsky Formation. Abbreviations: Is = saturation magnetization; Iso = saturation magnetization at room temperature; χ = magnetic susceptibility; χ_o = maximal magnetic susceptibility.

magnetite that resulted from the oxidation of pyrite grains. Both these secondary magnetite and altered titanomagnetite grains may be responsible for the low quality of the paleomagnetic record in some of the samples from the Arydzhangsky Formation.

The thermomagnetic curves for most samples of the Onkuchaksky Formation (Figure 3c) reveal Curie points in the temperature range 300–400 °C. These Curie points are consistent with electron microscope and microprobe observations showing abundant primary magmatic titanomagnetite grains with dendritic and cruciform quench structures. These structures are indicative of very rapid cooling of lavas, consistent with the observed Curie points, and it is an argument for a primary origin of the magnetization of the studied samples. In several measured samples traces of magnetic minerals with Curie points close to 580 °C (probably magnetite) and 100–120 °C (high titanium titanomagnetite) can also be seen.

4.1. Norilsk Region

Although the magnetic mineralogy of the Sunduk and the Ergalakh sections (Figures 3d and 3e) varies to some extent from formation to formation, the common and the most pronounced feature is the occurrence of a magnetic phase with Curie temperatures at 580–600 °C. Heunemann et al. (2004) observed a similar thermomagnetic behavior for other sections of the Norilsk region. They found the magnetic phase to be magnetite or titanium-poor titanomagnetite inside titanomagnetite grains deuterically oxidized during cooling between 900 and 500 °C. Such titanomagnetite grains are widespread in the samples from the Sunduk and the Ergalakh sections and, likely, contain the magnetic phase that carries the primary thermoremanent magnetization.

5. Paleomagnetism

All samples were thermally demagnetized up to 580–680 °C with an average of 12 steps to isolate the components of the natural remanent magnetization (NRM). The measurements were performed in the paleomagnetic laboratories of the Institut de Physique du Globe de Paris (France), Institute of Physics of the Earth (Moscow, Russia), and Lomonosov Moscow State University using a 2G Enterprises cryogenic magnetometer, JR-6 spinner magnetometers (AGICO), homemade nonmagnetic ovens in Paris, and MMTD80 thermal demagnetizer (Magnetic Measurements Ltd.) in Moscow.

The magnetic components were determined after inspection of orthogonal projections (Zijderveld, 1967) using principal component analysis (Kirschvink, 1980). Site mean directions based on 4 to 10 samples results were calculated using Fisher (1953) statistics. The entire paleomagnetic analysis was performed using the PaleoMac software (Cogné, 2003) and Enkin's (1994) paleomagnetic software packages.

The quality of the paleomagnetic record differs from flow to flow. In the Maymecha-Kotuy sections we observe the most clear paleomagnetic signal in the basalts of the Onkuchaksky Formation. Two components of NRM are isolated in most samples from the Onkuchaksky and the Arydzhangsky Formations. A low-temperature (LT) component, unblocked by heating at 200–250 °C, has a direction close to the modern geomagnetic field. We therefore consider this component to be a modern overprint and do not discuss it further. The second, HT component decays to the origin of an orthogonal vector diagram between 200 and 600 °C (Figure 4).

In addition to the LT and HT components, we observe in several samples from the three lowermost flows of the Onkuchaksky Formation an intermediate component (IC) with unblocking temperatures between 200 and 350 °C (Figure 4d, sample 123-08). Compared to the HT component, this component has a reverse polarity and its direction is virtually antipodal to that of the HT component. This IC could result from remagnetization during emplacement of the upper flows of the Truba section, which have reversed polarity, or it could originate from a partial self-reversal of magnetization (Gapeev & Gribov, 2008). Because we can observe within the same flows samples with both 2 (LT + HT) and 3 (LT + IC + HT) components and there is no dependence of the IC unblocking temperature range on stratigraphic position of the flows (i.e., on proximity to possible source of remagnetization), we prefer the second explanation that the reverse polarity component originates from partial self-reversal.

In the five flows from the lower part of the Onkuchaksky Formation (flow 6 through flow 11) most samples contain a very noisy paleomagnetic record that makes confident isolation of magnetization components difficult. Therefore, we have not used these data in calculating the mean paleomagnetic directions.

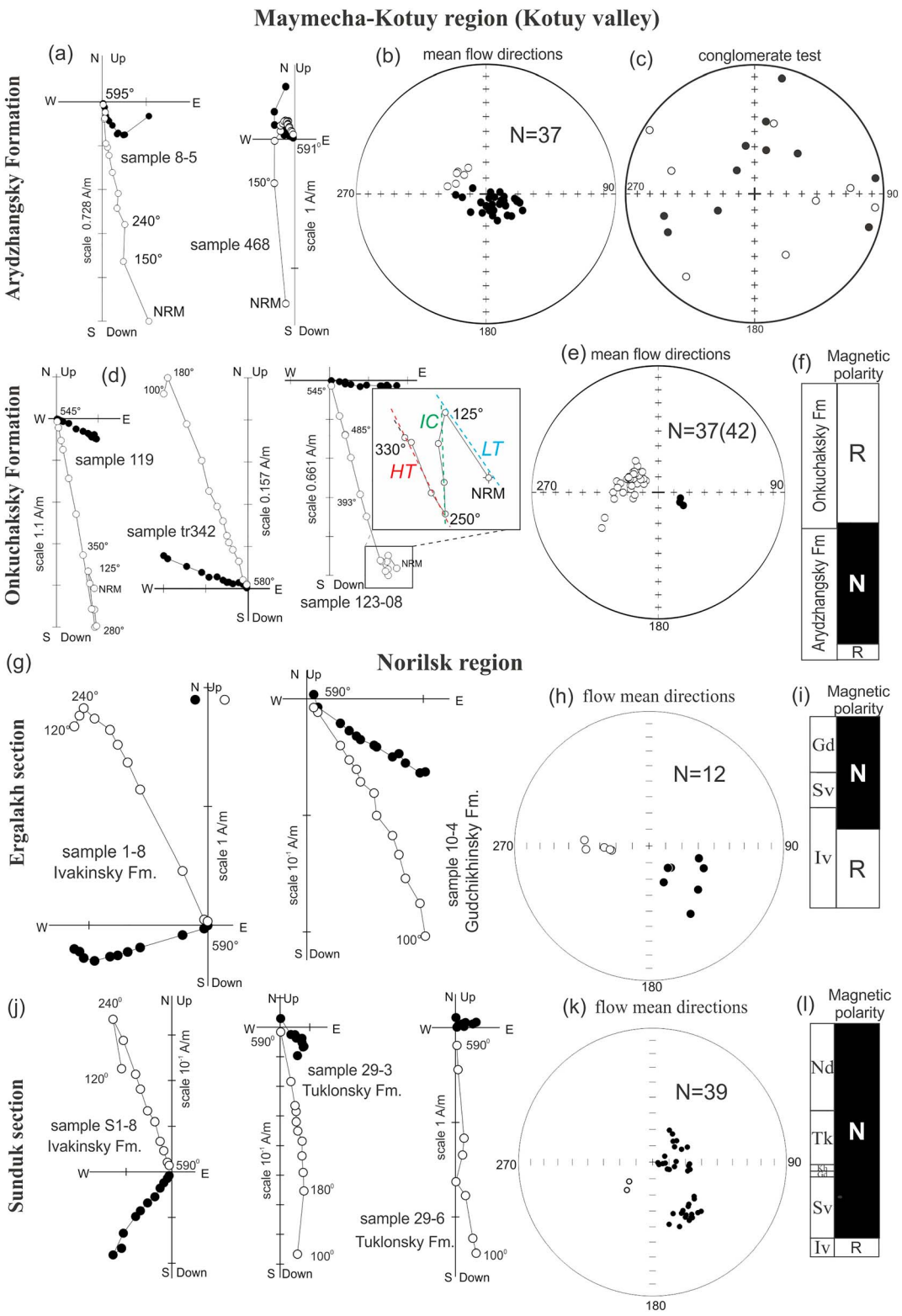

Figure 4. Paleomagnetism of trap formations of the Maymecha-Kotuy region (Kotuy river valley; a–f) and the Norilsk region (g–l). (a, d, g, and j) Orthogonal component plots; closed (open) circles represent projection onto the horizontal (vertical) plane. (b, e, h, and k) Equal area projections showing mean flow directions for (b) Arydzhangsky Formation, (e) Onkuchaksky Formation, (h) Ergalakh section, and (k) Sunduk section; closed (open) circles on the equal area net indicate down (up) direction. (c) Equal area projection representing positive result of conglomerate test in Arydzhangsky Formation. (f, i, and l) Magnetic polarity scales of volcanic traps of (f) the Kotuy river valley, (i) Ergalakh section, and (l) Sunduk section; black (white) = normal (reversed) polarity.

Nevertheless, we note that demagnetization plots for flow 6 through flow 11 clearly indicate reverse polarity of the HT component in these flows.

The paleomagnetic record in the rocks of the Arydzhangsky Formation is generally more challenging to interpret (Figure 4) than in the rocks of Onkuchaksky Formation. Nevertheless, we were able to isolate the HT component for virtually all the sampled flows. Unfortunately, due to the relatively low quality of the paleomagnetic record, in several of the flows we were not able to determine mean flow directions with the desired precision (supporting information).

Twenty samples of volcanic clasts were taken from the lava breccia in the lower part of the Arydzhangsky Formation (Medvezhya section). The HT component of magnetization (350–560 °C) was isolated in 19 of them; the distribution of this component on the samples level is shown on the Figure 4c. The positive result of conglomerate test ($R/R_0 = 2.33/6.98$, $N = 19$; Watson, 1956) indicates the primary origin of the HT component isolated in the Arydzhangsky Formation.

The mean directions of the isolated HT components calculated for each flow are shown in the supporting information and Figures 4b, 4e, 4h, and 4k. The lowermost part of the Arydzhangsky Formation (sometimes referred to as the Khardakhsky Formation) in the lower part of the composite Kotuy section has a reverse polarity (supporting information and Figure 4f). Above this, the greater part of the Arydzhangsky and the lowermost flows of the Onkuchaksky Formations yield normal polarity directions, while the overlying middle and upper parts of the Onkuchaksky Formation are again reversely magnetized. A reversal test (McFadden & McElhinny, 1990) applied to the whole section indicates some minor nonantipodality ($\gamma/\gamma_c = 8.5°/3.5°$) that could result either from insufficient averaging of the secular variation, or from weak contamination by the LT component.

Samples from the Sunduk and the Ergalakh sections (Norilsk region) also usually contain two components of NRM corresponding to LT and HT (Figures 4g and 4j). As in the Maymecha-Kotuy region, the LT component (with unblocking temperatures up to 250 °C) is interpreted to be of recent origin because of its similarity to direction of the modern geomagnetic field. After removal of the LT components only the HT component remains and persists until 580–600 °C. The mean directions of the HT component calculated for each flow of the studied section are shown in the supporting information and in Figures 4h and 4k. Several of the lowest flows in the Ivakinsky Formation in both the Sunduk and the Ergalakh sections yield a reverse polarity.

Although paleomagnetic data from the Siberian Traps have been used since early 1960s, any form of fold test to demonstrate their reliability has not been carried out until now because of the lack of dip in the trap volcanics, which lie virtually flat in all their localities studied early. However, in the marginal part of the Kharaelakh trough there is one well-exposed section (the "Mokulay creek section") where the volcanic rocks of the Morongovsky and the Mokulaevsky Formations dip at 30–35°, allowing implementation of the fold test. We studied the lava flows and tuffs of the Morongovsky Formation from this section, their data (isolated HT directions) are presented in Table 1. The mean directions calculated for rocks of the Morongovsky Formation from the Mokulay creek and Abagalakh (Gurevitch et al., 2004) sections are statistically similar ($\gamma/\gamma_c = 4.0°/7.5°$; McFadden & McElhinny, 1990) in the stratigraphic system of coordinates but differ significantly ($\gamma/\gamma_c = 34.0°/7.5°$) in the geographic coordinate system. This result constitutes a positive fold test and indicates a prefolding age for the HT component of magnetization. The dip of the Morongovsky section is believed to been acquired during the formation of the Kharaelakh trough, immediately after trap emplacement, and so the positive fold test unambiguously points to the primary nature of the HT component.

In summary, the primary origin of the HT component isolated in the studied rocks is supported by

1. the proximity of the measured mean directions to the expected PT directions for the Siberian craton (Pavlov et al., 2007), and their distinction from younger directions (Pavlov, 2012);
2. the positive conglomerate test for the Arydzhangsky Formation;
3. the fact that normal and reversed polarity directions are nearly antipodal;
4. the positive fold test for the Morongovsky Formation;
5. the existence of primary magmatic magnetic minerals;
6. and the presence in studied sections of DGs, whose mean paleomagnetic directions significantly differ (see below).

Table 1
Mean Paleomagnetic Directions for Flows and Tuffs Layers for Morongovsky Formation (Mokulay Section)

Flow	*N*	Dg (°)	Ig (°)	Ds (°)	Is (°)	*k*	α95 (°)
flow 1	5	194	83.7	83.1	60.9	93.9	7.9
tuff 1-2	5	158.9	74.4	99.2	54	151.8	6.2
flow 2	5	155.5	81.3	87.7	56	27.2	14.9
flow 3	5	185.6	69.6	112.3	60.3	49.9	10.9
tuff 3-4	4	209.6	64.8	125.5	69.1	167.6	7.1
flow 4	6	217.9	66.3	120	72.4	84.9	7.3
tuff 4-5	4	203.6	62.7	130.2	66.2	96.3	9.4
flow 5	6	208.7	67.3	118.5	68.6	39	10.9
flow 6	5	227.4	62.2	132.4	77.1	102.6	7.6
tuff 6-7	3	270.4	79.5	63.3	67.7	45	18.6
flow 7	6	230.6	68.7	104.4	75.7	31.1	12.2
flow 8	5	295.3	57.5	359.4	67.3	209.8	5.3
tuff 8-9	5	281.3	78	56.4	67.7	33.2	13.5
flow 9	5	275.6	70.8	43.7	73.8	35.2	13.1
tuff 9-10	5	255	61.8	51.7	85.9	36.2	12.9
flow 10	5	269.2	62	14.3	80.5	49.1	11
tuff 10-11	4	256.1	52.3	275.8	83.8	18.9	21.7
flow 11	5	251.2	57.9	170.9	89.6	21.2	17
flow 12	4	246.5	41.7	237.5	73.3	50.2	13.1
flow 13	5	228.2	41.2	199.8	67.4	130.8	6.7
flow 14	5	230.1	47.3	191.6	73.1	90.1	8.1
flow 15	6	209.8	37.7	179.9	56	118.6	6.2
MEAN for Mokulay section	22	234.0	66.5	108.9	78.1	18.8	7.3
MEAN for Abagalakh section (Gurevitch et al., 2004)	22	19.5	78.0	90.5	80.0	164.0	3.6

Note. *N* = number of samples; Dg, Ig = declination and inclination in geographic coordinates; Ds, Is = declination and inclination in stratigraphic coordinates; *k* = concentration parameter; α95 = radius of confidence circle.

In addition, the similarity of unblocking temperature spectra of laboratory induced thermoremanent magnetization and the HT component (Shcherbakova et al., 2013) can be considered as evidence for its thermoremanent nature, and therefore for its primary origin.

6. Discussion

The question of how much time is recorded in a given paleomagnetic DG is critical to our interpretations. The Holocene period provides a high-resolution record of variations in the Earth's magnetic field. We use the CALS10k.1b global model of the Earth's magnetic field (M. Korte et al., 2011) to generate the expected secular variation for a site located at high latitude (70°N, 90°E), which corresponds to the latitude of the Siberian Traps at the PT boundary. The secular variation that we obtain is generally less than 2° per century with the exception of the last four centuries where it exceeds 8° per century. We then estimate the angular distance between two values on this secular variation curve separated by a fixed time interval. For that purpose, we use a Monte Carlo routine, which randomly picks 2,000 points of the secular variation curve separated from each other by an age interval varying from 100 to 1,800 years. We calculate the angular distances that encompass 50% and 95% of the estimates respectively (Figure 5a). The angular distance rises rapidly for the shortest time intervals. The 95% (50%) threshold yields a distance of 4.2° (1.8°) for a time interval of 400 years. These estimates provide a measure of the elapsed time within a volcanic pulse. The validity of these estimates is based on the secular variation rates inferred from the CALS10k.1b global model being appropriate for the Permian-Triassic. Plateaus observed on the angular distance at time intervals greater than 700–800 years are likely linked with the duration spanned by the CALS10k.1b model, precluding an estimate of the minimum time interval between single eruptive events. The angular distance is less than 5° in 95% of cases (Figure 5b) and generally corresponds to an interval of time of about 400 years (95% threshold) based on our estimates (Figure 5a). Overall, this exercise supports our assumption that 300–400 years can be considered as a maximum estimate for the duration of a set of flows erupted within a single, statistically indistinguishable DG.

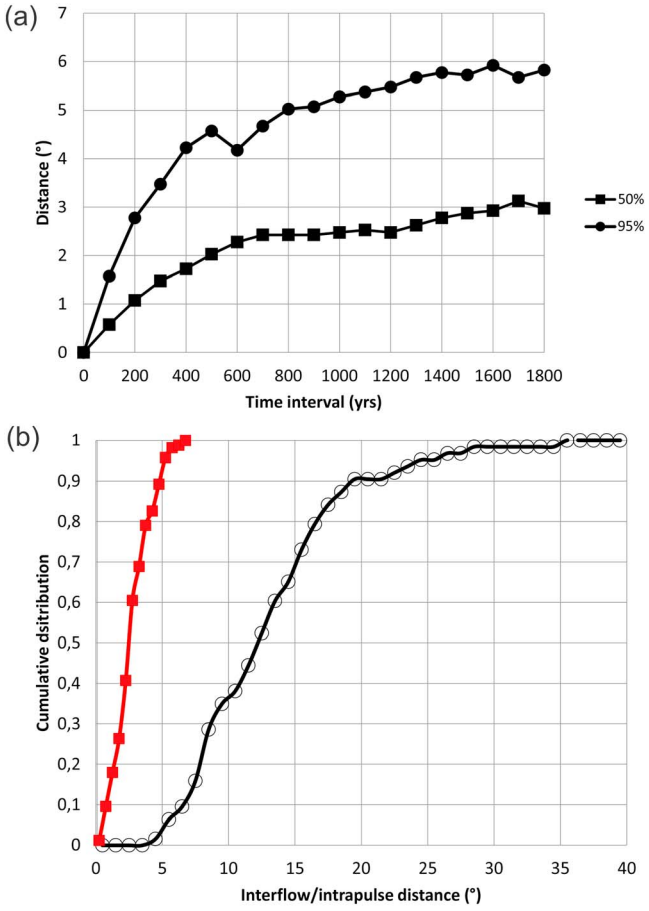

Figure 5. (a) Distance between two points in function of time interval (1,000 trials) within the secular variation curve calculated with the Calc10k.1b global model (M. Korte et al., 2011). (b) Cumulative distribution of distance between: Site mean direction belonging to DG and mean direction of DG (red); mean directions of consecutive ID, consecutive DG, and consecutive DG and ID (black). DG = directional group; ID = individual direction.

Seventeen DGs and 13 IDs were identified in the composite section on the Kotuy River, consisting in total of 79 volcanic units (Figure 6 and the supporting information). If our assumption that DGs were emplaced over a maximum time interval of 300–400 years is valid, we estimate the total duration of volcanic activity for the composite Kotuy River section as at most 7,000–8,000 years.

Using the same procedure for the Norilsk lavas, 4 DGs and 3 IDs were identified in the Ergalakh section, and 9 DGs and 6 IDs in the Sunduk section. Twenty-three DGs and 12 IDs were found in the composite Norilsk section (76 lava flows) comprising the Listvjanka, Icon, and Abagalakh sections studied by (Heunemann et al., 2004; Figure 6 and the supporting information). In total, according to the time constraints for DGs and individual lavas discussed above, the duration of active volcanism that produced the Norilsk composite section did not exceed 10,000–11,000 years. In our analysis we did not consider the Talnakh section, studied by Heunemann et al. (2004), because it is located very close to the Listvjanka section and repeats the lower part of this section.

Our duration estimates do not include potential hiatuses between volcanic eruptions. However, the absence of substantial paleosols and/or weathering crusts between the flows suggests that periods between eruptions were short. It is possible that dry, cold conditions expected at 50° to 60° north latitude may have slowed the formation of sediments or soils during emplacement of Siberian Traps lavas.

The high values of the Non-Random-Ordering (NRO) factor (Biggin et al., 2008) calculated for the composite Kotuy and Norilsk sections (NRO = 0.9999) constitute further evidence for the absence of long periods between volcanic pulses. The NRO factor is a measure of serial correlation of the flow mean directions in the lava sequences. Calculated high NRO values point to a high correlation of paleomagnetic directions among consecutive lava flows and, therefore, indicate brief time gaps between their eruptions.

The detailed paleomagnetic data from the Norilsk lava flows provide additional constraints on the duration of volcanic activity of this region. Heunemann et al. (2004) and Gurevitch et al. (2004) identified in the Norilsk composite section (Listvjanka, Icon, and Abagalakh sections, overall thickness ~2,200 m) reversed (R), transitional (T), excursional (E), and normal (N) paleomagnetic intervals. Between the transitional and excursional intervals (flows gd2-5, tk6-7) the geomagnetic field briefly reached normal polarity. The authors further suggest that the excursional interval may correspond to a post-transitional rebound effect (Valet et al., 2012).

Our results reveal the same features in the Sunduk section, which contains almost all (Figures 6 and 7) of the intervals identified in the Norilsk composite section by Heunemann et al. (2004). The lowermost reverse polarity interval of the Sunduk section includes two flows, corresponding to DG1S (the letter after the DG is used to indicate the section; in this case the Sunduk section). The next 17 flows (ID1S, DG2S, DG3S, DG4S, and DG5S) are the transitional interval. Excursional directions, identified as Heunemann et al. (2004) and Gurevitch et al. (2004) did, are recorded by flows in DG8S and ID6S.

Similar to the data from Heunemann et al. (2004), in the Sunduk section between the transitional and excursional intervals we observe several flows (C20S-C31S) containing DGs and IDs (DG6S-DG7S and ID2S-ID5S), which mark the first arrival of the geomagnetic field into a “precursor” normal state, succeeded by a possible posttransitional excursion (DG8S, ID6S, DG9S[?]). The uppermost three flows (DG9S), possibly, contain the record of the final arrival of the field to a stable (normal) state. In the Ergalakh section the reverse and transitional intervals can be identified (levels DG1E, DG2E and ID1E, ID2E, ID3E, and DG4E, respectively).

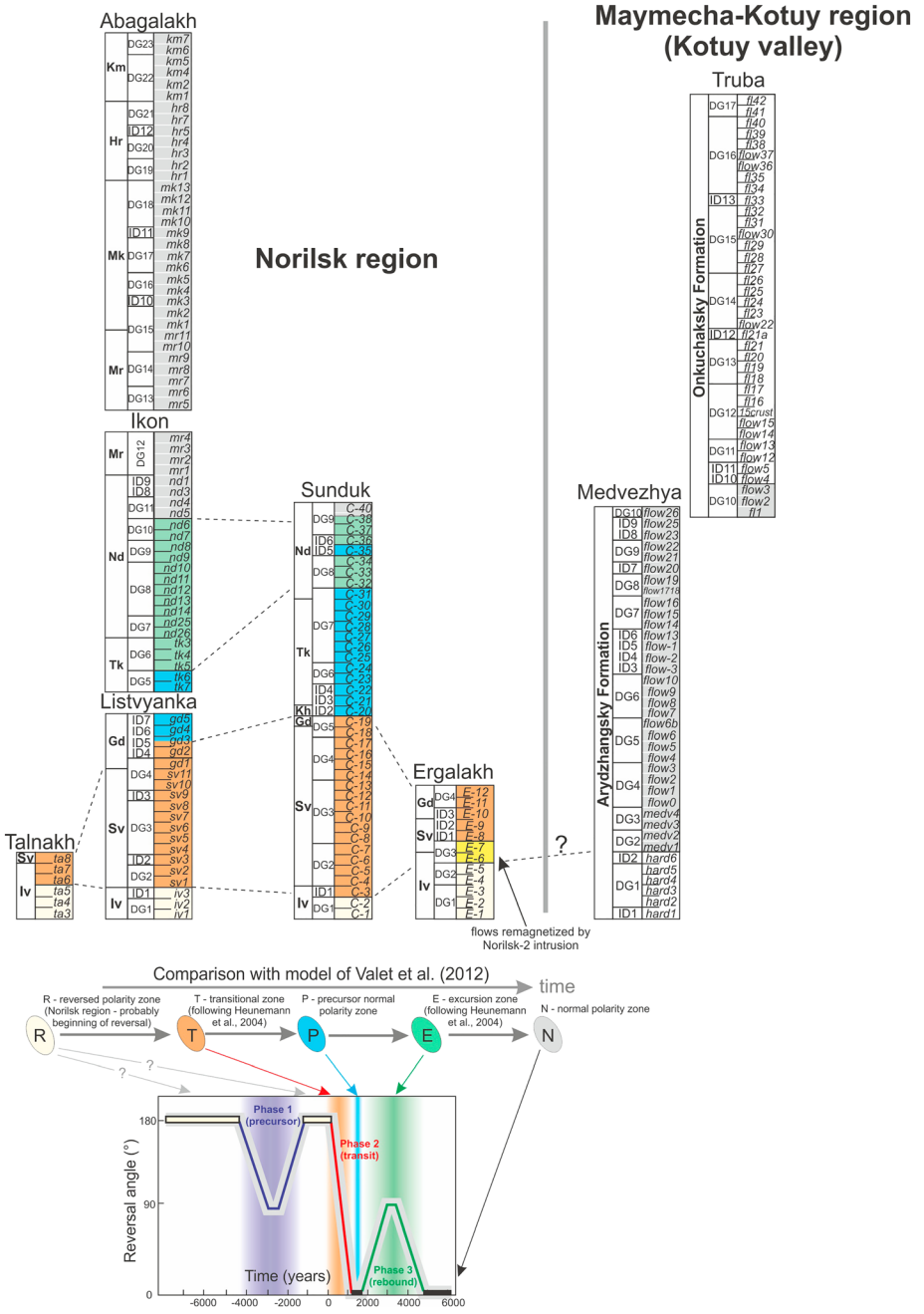

Figure 6. Magnetic stratigraphy of the Kotuy and Norilsk regions sections. Correlation of the Norilsk region section and comparison of their magnetostratigraphic record with the model of the geomagnetic reversal stages of Valet et al. (2012). DG = directional groups; ID = individual directions. Formations: Iv = Ivakinsky; Sv = Syverminsky; Gd = Gudchikhinsky; Kh = Khakanchansky; Tk = Tuklonsky, Nd = Nadezhdinsky; Mr = Morongovsky; Mk = Mokulaevsky; Kh = Kharaelakhsky; Km = Kumginsky; Sm = Samoedsky; Ar = Arydzhangsky; On = Onkuchaksky. To simplify the figure, directional groups are denominate without indication of sections.

Based on the analysis of several well-recorded reversals of different ages, Valet et al. (2012) have identified three phases during magnetic reversals: a precursor, a transit, and a rebound phase. The typical timescales for these phases can be used to place additional constraints on the timescales represented by the transitional and excursional intervals in the Norilsk composite section (Figures 6 and 7). In the case of the Norilsk lava flows, only the transit and rebound phases are present, and, following Valet et al. (2012), their total duration may have not exceeded 1 and 2.5 kyr, respectively. Here we assume these phases are related to the same

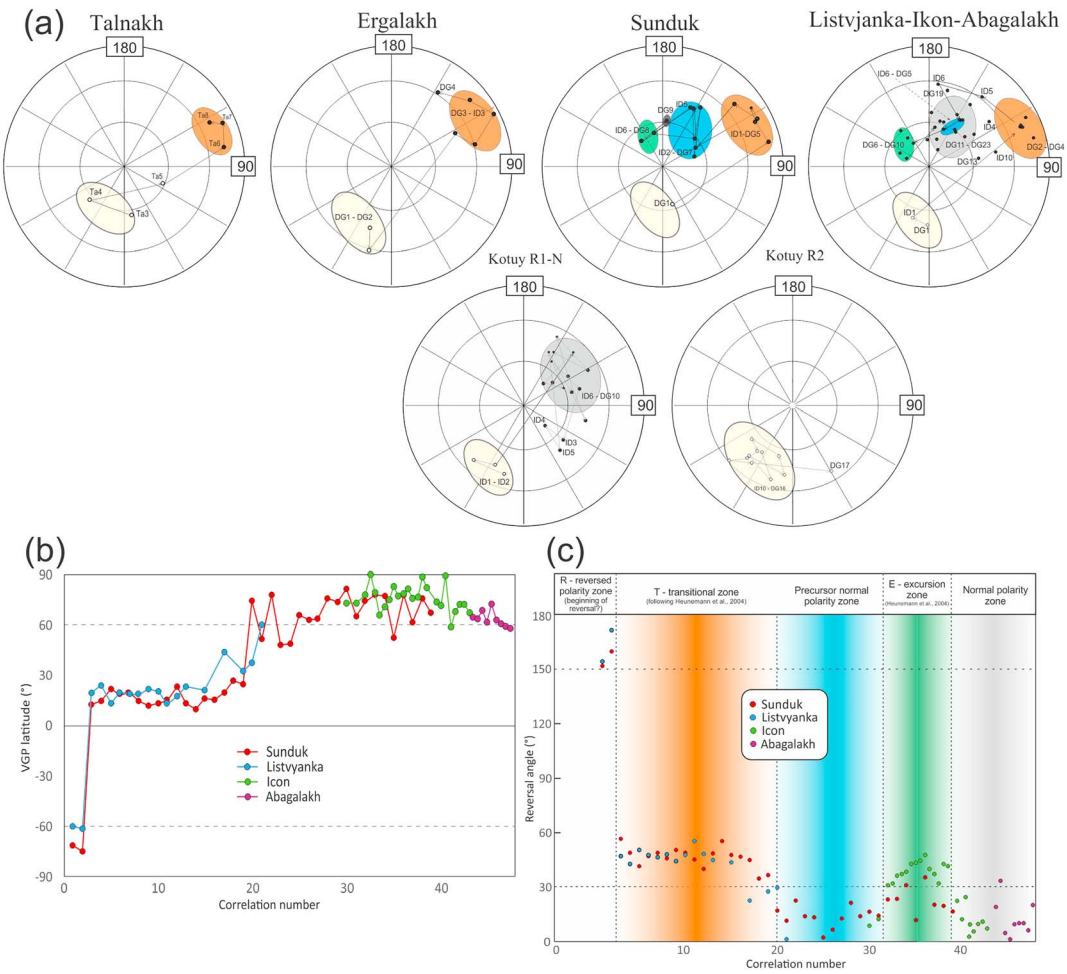

Figure 7. (a) Virtual geomagnetic poles (VGPs) sequences for the Kotuy and Norilsk regions sections. The color of the ovals corresponds to the reversal stages according to Figure 6. (b, c) Comparison with the model of Valet et al. (2012): (b) VGP latitudes and (c) reversal angles between each successive direction and the local direction of the present geocentric axial dipole field in each sequence of lava flows.

reversal event, though we cannot completely exclude the possibility that the observed transitional and excursional intervals are linked to separate geomagnetic events. On this basis, we conclude that at least one quarter or even one third of the Norilsk effusive lavas (totaling ~1,000 m in thickness) was likely formed during a relatively short time interval, corresponding to the duration of a reversal of the geomagnetic field.

The transitional interval of the Norilsk trap sections, corresponding to the Syverminsky and Gudchikhinsky Formations, is characterized by paleomagnetic directions with on average shallower inclinations than those of the overlying intervals (e.g., $I = 48–59°$ for the transitional interval in the Listvjanka section and $I = 72–81°$ for the stable normal interval in the Icon section). The latter gives us the tool to determine the same transitional interval in borehole data.

Indeed, in two out of the three paleomagnetically studied boreholes (Gurevitch et al., 2004; Mikhal'tsov et al., 2012) that crossed the Gudchikhinsky and Syverminsky Formations (CD28 and HS59; see Figure 1), the mean inclinations, calculated for these formations, are close to those obtained for the transitional interval (Heunemann et al., 2004; Gurevitch et al., 2004) and, at a 95% level of confidence, are shallower than the mean inclinations calculated for overlying formations.

Therefore, a magmatic event corresponding to the described transitional interval can be traced over a large region, including at least the Kharaelakh, Norilsk, and Imangda troughs, and about 20,000 km^3 of the lava (a

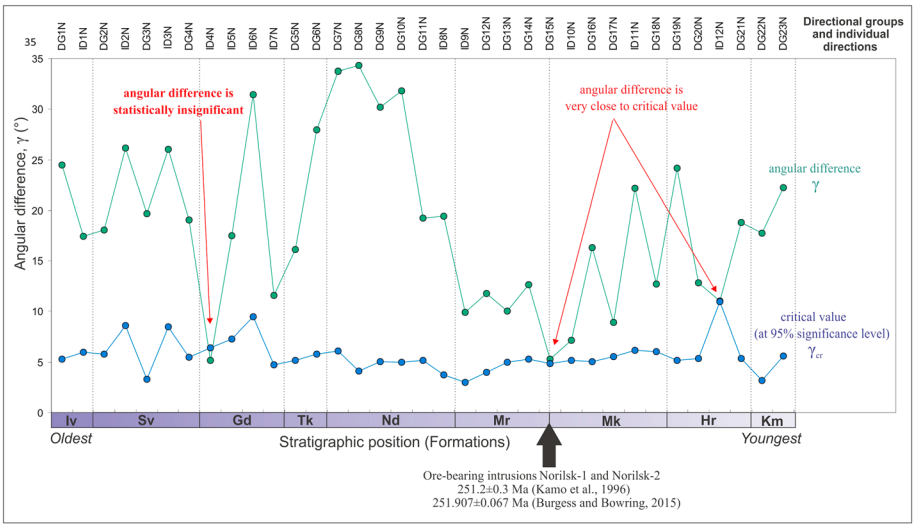

Figure 8. Comparison of paleomagnetic directions of the Norilsk composite section (Listvjanka + Icon + Abagalakh) with the paleomagnetic direction of the intrusion Norilsk-2. Green circles stand for angular difference between comparing directions; blue ones show corresponding 95% confidence values. When a green circle is located above corresponding blue one, angular difference is statistically meaningful and vice versa. DG = directional group; ID = individual direction.

minimum volume estimate for the effusive lava flows of the Syverminsky and Gudchikhinsky Formations based on existing outcrop extent) was erupted during only a few volcanic pulses and individual eruptions.

We have also obtained a paleomagnetic direction from the ore-bearing Norilsk-2 intrusion that cuts flows E6 and E7 in the Ergalakh section. The paleomagnetic directions of flows near the intrusion are indistinguishable from that of the intrusion and statistically different from the other flows of the Ergalakh section (supporting information). The flows, therefore, may have been remagnetized by the Norilsk-2 intrusion. If so, then the average of the paleomagnetic directions of the two flows and the intrusion gives a more accurate estimation for the direction of the geomagnetic field of the time of emplacement of this intrusion (GFN2I) and allows a comparison with the paleomagnetic directions of volcanic pulses and individual flows isolated in the composite section (Listvjanka + Icon + Abagalakh) of the Norilsk region.

This comparison bears on the outstanding question of the link between the unique ore-bearing Norilsk-type intrusions (including considered to be coeval Norilsk-2 and Norilsk-1 intrusions; Naldrett, 2003) and the flood basalts. While some workers consider these intrusions to be comagmatic with the basalts of the Morongovsky (Fedorenko, 1994) or Mokulaevsky (Naldrett, 2003) formations, Czamanske et al. (1994) conclude that none of the intrusions are comagmatic with any of the lavas. Latypov (2002) also claimed that the Norilsk-type intrusions have no comagmatic volcanic rocks in the Norilsk region and further suggested that the spatial association of these intrusions with the flood basalts is likely coincidental rather than genetic. If this is true, then the age of the Norilsk-1 intrusion cannot be directly used to estimate the age of the main Norilsk lava emplacement (Burgess & Bowring, 2015; Kamo et al., 1996).

A comparison of the paleomagnetic directions obtained for the Norilsk-2 intrusion (GFN2I) with the lavas of the Norilsk composite section (Figure 8) reveals only one level (ID4N) that has a paleomagnetic direction statistically indistinguishable from GFN2I, along with two levels (ID12N and DG15N) with directions that are very close to direction GFN2I.

The mean directions of two of these levels (ID4 and ID12) are obtained from individual flows and their similarity to the direction of GFN2I may be coincidental. DG15, however, comprises four consecutive flows. The close match between their paleomagnetic directions and that of GFN2I is highly unlikely to be coincidental and, therefore, is suggestive that they are coeval or nearly coeval. Thus, we conclude that the ore-bearing Norilsk intrusions and lavas of the uppermost Morongovsky and lowermost Mokulaevsky Formations are very close in age and, therefore, possibly have a genetic relation, in agreement with Fedorenko (1994) and Naldrett (2003).

Table 2
Estimates of Amplitudes of Secular Variations Recorded in the Studied Sections

	Cutoff according to Vandamme (1994)				Cutoff 45°			
Used data	*n*/*N*	Sb	Sb lower	Sb upper	*n*/*N*	Sb	Sb lower	Sb upper
All mean flow directions	49/54	17.0	15.0	19.0	50/54	17.9	15.4	20.5
Mean flow directions with $k > 50$	44/48	17.1	14.9	19.3	46/48	18.9	16.1	21.8
Mean flow directions with $k > 100$	28/29	17.0	14.1	19.8	29/29	18.4	14.8	22.1

Note. *n*/*N* = number of mean flow directions used in statistics/total; Sb = virtual geomagnetic pole scatter according to McElhinny and McFadden (1997); Sb lower, Sb upper = confidence interval; *k* = concentration parameter.

Furthermore, this result has important implications for the evolution of the magmatic chambers during the emplacement of Norilsk ore-bearing intrusions and volcanic flows. Some models of the Cu-Ni-Pt deposits genesis suggest that the ore-bearing intrusions were derived from the parental magma of the Nadezhdinsky Formation, based on the depletion in chalkophile elements in the Nadezhdinsky lavas (Lightfoot & Keays, 2005). If this idea is true, we can estimate the time gap between the initial enrichment of magma in chalkophile elements and the emplacement of sulfide-rich intrusions. Since the uppermost Nadezhdinsky flows are separated from the Morongovsky-Mokulaevsky boundary by three DGs, this time interval could not be shorter than 1–2 kyr.

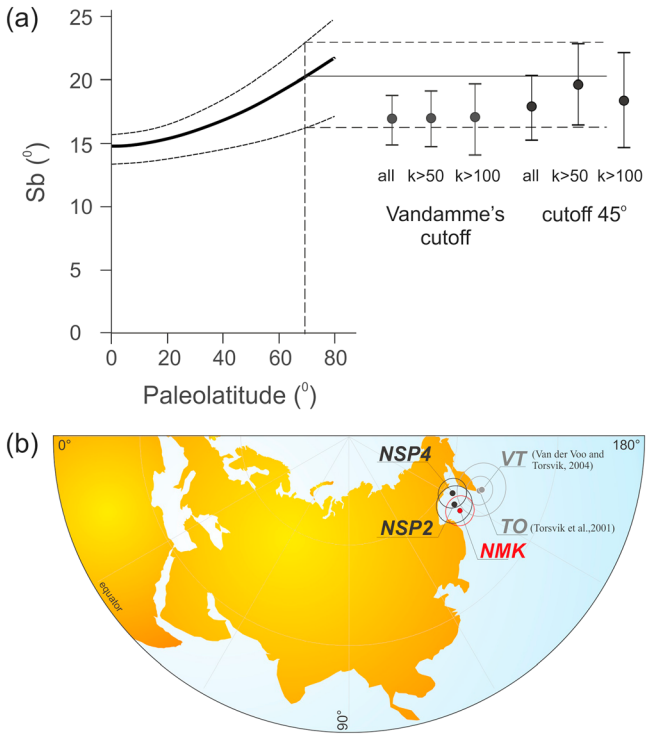

Figure 9. (a) Secular variations at the Permian-Triassic boundary as inferred from obtained data (black dots and corresponding error bars; Table 2) and their comparison with latitude dependence suggested by Biggin et al. (2008) on the basis of data, compiled by Johnson et al. (2008) for last 5 million years. Dashed curves represent 95% uncertainty. (b) Comparison of refined pole position (Norilsk-Maymecha-Kotuy, NMK) with location of previously suggested PT Siberian (NSP2 and NSP4: Pavlov et al., 2007) and European paleomagnetic poles (TO: Torsvik et al., 2001; VT: van der Voo & Torsvik, 2004). European poles are shown just for illustration; their comparison with new obtained PT Siberian pole lies beyond the scope of this paper.

Our data further suggest that the age obtained by Kamo et al. (1996; 251.1 ± 0.3 Ma) or, recently, by Burgess and Bowring (2015; 251.907 ± 0.067 Ma) on the Norilsk-1 intrusion should be considered to be close to the age of the boundary between the Morongovsky and Mokulaevsky Formations.

The results obtained in this study allow the calculation of the VGP scatter. To assure the independence of constituent data, only DG and ID mean directions were used. We then discarded those mean directions that correspond to transitional and excursional intervals and to levels between them. Thus, only mean directions coming from reverse and normal intervals have been used for our calculation: in total, we used the mean directions of 54 DGs and IDs derived from 123 volcanic flows from 7 different sections. After applying the Vandamme's cutoff method (Vandamme, 1994), five VGP's were rejected and the final calculation yielded the values 15.7° (95% confidence interval 13.3°/17.8°) for the composite Kotuy section, 17.4° (95% confidence interval 13.7°/20.8°)—for the Norilsk composite section, and 17.0° (95% confidence interval 15.0°/19.0°; see Table 2)—for both the sections taken together. If, instead of applying of Vandamme's method, we use (again for both these sections) fixed 45° cutoff angle (similarly to, e.g., Johnson et al., 2008), we get the Sb estimate (17.9°, with 95% confidence interval 15.3°/20.3°; see Table 2), which is close to previous one.

In several studies (e.g., Biggin et al., 2008) the authors use in their paleosecular variation analysis only mean directions with Fisher precision parameters (Fisher, 1953) $k > 50$ or $k > 100$. To make our results compatible with results of these studies, we also calculated Sb using only data coming from flow mean directions with $k > 50$ and $k > 100$. The result of these calculations are presented in the Table 2.

As shown on Figure 9a, the value calculated for the amalgamated Norilsk and Kotuy data set fits well with values expected from latitude dependence suggested by Biggin et al., 2008 on the basis of data compiled by Johnson et al., 2008 for last 5 million years.

Thus, our results indicate that geomagnetic field variations at the PT boundary were (at least at high latitude) comparable to those during the latest Cenozoic.

The same data set can be used for the calculation of a refined Siberian PT paleomagnetic pole. The most recent estimate for the overall mean paleomagnetic pole of the Siberian Traps (poles NSP2 and NSP4; Pavlov et al., 2007) is derived from highly heterogeneous data coming from volcanic flows, sills, dykes, and remagnetized sedimentary rocks. Moreover, different sampling policies were used in the studies that produced these data. Our calculation is based exclusively on volcanic flows. The new refined pole Norilsk-Maymecha-Kotuy (NMK) has the coordinates: PLat = 52.9°, PLong = 147.1°, with a radius of confidence circle A95 = 4.3°, precision parameter $K = 23.2$, and $N = 49$ (Figure 9b).

7. Conclusions

1. Detailed paleomagnetic studies of the most representative sections of the Permian-Triassic traps of the northern Siberian platform indicate that volcanic activity in the Norilsk and Maymecha-Kotuy regions occurred during a limited number of high-volume volcanic pulses and individual eruptions rather than in flows emplaced at regular intervals over the lifespan of the LIP. For the composite Kotuy River section, we identify 17 DGs corresponding to volcanic pulses and 13 IDs corresponding to individual eruptions. For the Norilsk composite section, we identify 23 DGs corresponding to volcanic pulses and 12 IDs corresponding to individual eruptions. This implies that the total duration of volcanic activity in the Maymecha-Kotuy and Norilsk regions did not exceed a time interval of the order of 10,000 years. This estimation does not include the periods of lulls between volcanic events, but the absence of sedimentary layers and weathering crusts in the studied sections implies that volcanic lulls were brief. This inference is also supported by the high value of the NRO factor.
2. We confirm the presence of the thick transitional and excursional intervals in the Norilsk trap sections, as suggested by Heunemann et al. (2004) and Gurevitch et al. (2004). These intervals can be traced across the entire Norilsk region. This may indicate that at least from one quarter to one third of the Norilsk region volcanic sequence (perhaps more than 1,000 m in thickness) was formed within several thousand years or less, based on the typical timescales of magnetic transitions and excursions. Tracing the transitional interval through the Kharaelakh, Norilsk and Imangda troughs, along with subdivision of sections suggested in this study, implies that more than 20,000 km^3 of lava may have been formed by just a few volcanic pulses and individual eruptions.
3. Our data suggest that the ore-bearing Norilsk-type intrusions are coeval or nearly coeval with the boundary of the Morongovsky and Mokulaevsky Formations.
4. A refined Siberian Permian-Triassic paleomagnetic pole Norilsk-Maymecha-Kotuy (NMK) based on data, coming exclusively from volcanic flows, is PLat = 52.9°N, PLong = 147.1°E, A95 = 4.3°, $K = 23.2$, and $N = 49$.
5. The geomagnetic field variations at the PT boundary were about the same as during the latest Cenozoic.

Acknowledgments
We thank Richard Ernst and John Geissman for their comments that greatly improved our manuscript. This work was supported by the U.S. National Science Foundation «The Siberian flood basalts and the end-Permian Extinction» (EAR-0807585), by the Russian Foundation for Basic Research (projects 16-35-60114, 18-05-70094 and 18-35-20058), and the projects of the Ministry of Education and Science of the Russian Federation (grants 14.Z50.31.0017 and 14.Y26.31.0029). This is IPGP contribution 4004. B.A.B. acknowledges support from NSF grant 1615147. All raw data used in this study are presented in the manuscript and in the supporting information.

References

Batt, C. M., Brown, M. C., Clelland, S.-J., Korte, M., Linford, P., & Outram, Z. (2017). Advances in archaeomagnetic dating in Britain: New data, new approaches and a new calibration curve. *Journal of Archaeological Science*, *85*, 66–82. https://doi.org/10.1016/j.jas.2017.07.002

Biggin, A. J., van Hinsbergen, D. J. J., Langereis, C. G., Straathof, G. B., & Deenen, M. H. L. (2008). Geomagnetic secular variation in the Cretaceous Normal Superchron and in the Jurassic. *Physics of the Earth and Planetary Interiors*, *169*(1-4), 3–19. https://doi.org/10.1016/j.pepi.2008.07.004

Black, B. A., Elkins-Tanton, L. T., Rowe, M. C., & Peate, I. U. (2012). Magnitude and consequences of volatile release from the Siberian Traps. *Earth and Planetary Science Letters*, *317-318*, 363–373. https://doi.org/10.1016/j.epsl.2011.12.001

Black, B. A., Weiss, B. P., Elkins-Tanton, L. T., Veselovskiy, R. V., & Latyshev, A. (2015). Siberian Traps volcaniclastic rocks and the role of magma-water interactions. *Bulletin of the Geological Society of America*, *127*(9–10), 1437–1452. https://doi.org/10.1130/B31108.1

Black, B., Neely, R., Lamarque, J. F., Elkins-Tanton, L. T., Kiehl, J. T., Shields, C. A., et al. (2018). Systemic swings in end-Permian climate from Siberian Traps carbon and sulfur outgassing. *Nature Geoscience*, *11*(12), 949. https://doi.org/10.1038/s41561-018-0261-y

Blackburn, T. J., Olsen, P. E., Bowring, S. A., McLean, N. M., Kent, D. V., Puffer, J., et al. (2013). Zircon U-Pb geochronology links the end-Triassic extinction with the central Atlantic magmatic province. *Science*, *340*(6135), 941–945. https://doi.org/10.1126/science.1234204

Buchan, K. L., & Ernst, R. E. (2019). Giant circumferential dyke swarms: Catalogue and characteristics. In R. K. Srivastava, R. E. Ernst, & P. Peng (Eds.), *Dyke swarms of the World: A modern perspective, Springer Geology* (pp. 1–44). Springer Nature Singapore. https://doi.org/10.1007/978-981-13-1666-1_1

Burgess, S. D., Bowring, S., & Shen, S. (2014). High-precision timeline for Earth's most severe extinction. *Proceedings of the National Academy of Sciences*, *111*(9), 3316–3321. https://doi.org/10.1073/pnas.1317692111

Burgess, S. D., & Bowring, S. A. (2015). High-precision geochronology confirms voluminous magmatism before, during, and after Earth's most severe extinction. *Science Advances*, *1*(7). https://doi.org/10.1126/sciadv.1500470

Burgess, S. D., Muirhead, J. D., & Bowring, S. A. (2017). Initial pulse of Siberian Traps sills as the trigger of the end-Permian mass extinction. *Nature Communications*, *8*(1), 164. https://doi.org/10.1038/s41467-017-00083-9

Chenet, A. L., Courtillot, V., Fluteau, F., Gérard, M., Quidelleur, X., Khadri, S. F. R., et al. (2009). Determination of rapid Deccan eruptions across the Cretaceous-Tertiary boundary using paleomagnetic secular variation: 2. Constraints from analysis of eight new sections and synthesis for a 3500-m-thick composite section. *Journal of Geophysical Research*, *114*, B06103. https://doi.org/10.1029/2008JB005644

Chenet, A. L., Fluteau, F., Courtillot, V., Gérard, M., & Subbarao, K. V. (2008). Determination of rapid Deccan eruptions across the Cretaceous-Tertiary boundary using paleomagnetic secular variation: Results from a 1200-m-thick section in the Mahabaleshwar escarpment. *Journal of Geophysical Research*, *113*, B04101. https://doi.org/10.1029/2006JB004635

Cogné, J. P. (2003). PaleoMac: A Macintosh™ application for treating paleomagnetic data and making plate reconstructions. *Geochemistry, Geophysics, Geosystems*, *4*(1), 1007. https://doi.org/10.1029/2001GC000227

Courtillot, V. E., & Renne, P. R. (2003). On the ages of flood basalt events. *Comptes Rendus Geoscience*, *335*(1), 113–140. https://doi.org/10.1016/S1631-0713(03)00006-3

Cox, A. (1970). Latitude dependence of the angular dispersion of the geomagnetic field. *Geophysical Journal of the Royal Astronomical Society*, *20*(3), 253–269. https://doi.org/10.1111/j.1365-246X.1970.tb06069.x

Czamanske, G. K., Wooden, J. L., Zientek, M. L., Fedorenko, V. A., Zen'ko, T. E., Kent, J., et al. (1994). Geochemical and isotopic constraints on the petrogenesis of the Norilsk-Talnakh ore-forming system. *Proceedings of the Sudbury-Norilsk symposium. Ontario Geological Survey Special Publication*, *5*, 313–342.

Enkin, R. J. (1994). A computer program package for analysis and presentation of paleomagnetic data. *Pacific Geoscience Centre, Geological Survey of Canada* (p. 16).

Fedorenko, V., & Czamanske, G. (1997). Results of new field and geochemical studies of the volcanic and intrusive rocks of the Maymecha-Kotuy area, Siberian Flood-Basalt Province, Russia. *International Geology Review*, *39*(6), 479–531. https://doi.org/10.1080/00206819709465286

Fedorenko, V., Czamanske, G., Zen'ko, T., Budahn, J., & Siems, D. (2000). Field and geochemical studies of the melilite-bearing Arydzhangsky Suite, and an overall perspective on the Siberian alkaline-ultramafic flood-volcanic rocks. *International Geology Review*, *42*(9), 769–804. https://doi.org/10.1080/00206810009465111

Fedorenko, V. A. (1994). Evolution of magmatism as reflected in the volcanic sequence of the Norilsk region. In P. C. Lightfoot & A. J. Naldrett (Eds.), *Proceedings of the Sudbury-Norilsk Symposium* (Vol. 5, pp. 171–183). Ontario Geological Survey Special Publication.

Fisher, R. (1953). Dispersion on a sphere. *Proceedings of the Royal Society of London. Series A: Mathematical and Physical Sciences*, *217*(1130), 295–305. https://doi.org/10.1098/rspa.1953.0064

Gallet, Y., Genevey, A., & Le Goff, M. (2002). Three millennia of directional variation of the Earth's magnetic field in western Europe as revealed by archeological artefacts. *Physics of the Earth and Planetary Interiors*, *131*(1), 81–89. https://doi.org/10.1016/S0031-9201(02)00030-4

Gapeev, A. K., & Gribov, S. K. (2008). Magnetic properties of intrusive traps of the Siberian platform: Evidence for a self-reversal of the natural remanent magnetization. *Izvestiya Physics of the Solid Earth*, *44*(10), 822–838. https://doi.org/10.1134/S1069351308100108

Gurevitch, E. L., Heunemann, C., Rad'ko, V., Westphal, M., Bachtadse, V., Pozzi, J. P., & Feinberg, H. (2004). Palaeomagnetism and magnetostratigraphy of the Permian–Triassic northwest central Siberian Trap Basalts. *Tectonophysics*, *379*(1-4), 211–226. https://doi.org/10.1016/j.tecto.2003.11.005

Heunemann, C., Krasa, D., Soffel, H., Gurevitch, E., & Bachtadse, V. (2004). Directions and intensities of the Earth's magnetic field during a reversal: Results from the Permo-Triassic Siberian trap basalts, Russia. *Earth and Planetary Science Letters*, *218*(1-2), 197–213. https://doi.org/10.1016/S0012-821X(03)00642-3

Jarboe, N. A., Coe, R. S., Renne, P. R., Glen, J. M. G., & Mankinen, E. A. (2008). Quickly erupted volcanic sections of the Steens Basalt, Columbia River Basalt Group: Secular variation, tectonic rotation, and the Steens Mountain reversal. *Geochemistry, Geophysics, Geosystems*, *9*, Q11010. https://doi.org/10.1029/2008GC002067

Johnson, C. L., Constable, C. G., Tauxe, L., Barendregt, R., Brown, L. L., Coe, R. S., et al. (2008). Recent investigations of the 0–5 Ma geomagnetic field recorded by lava flows. *Geochemistry, Geophysics, Geosystems*, *9*, Q04032. https://doi.org/10.1029/2007GC001696

Kamo, S. L., Czamanske, G. K., Amelin, Y., Fedorenko, V. A., Davis, D. W., & Trofimov, V. R. (2003). Rapid eruption of Siberian flood-volcanic rocks and evidence for coincidence with the Permian-Triassic boundary and mass extinction at 251 Ma. *Earth and Planetary Science Letters*, *214*(1-2), 75–91. https://doi.org/10.1016/S0012-821X(03)00347-9

Kamo, S. L., Czamanske, G. K., & Krogh, T. E. (1996). A minimum U-Pb age for Siberian flood-basalt volcanism. *Geochimica et Cosmochimica Acta*, *60*(18), 3505–3511. https://doi.org/10.1016/0016-7037(96)00173-1

Kirschvink, J. L. (1980). The least-square line and plane and the analysis of paleomagnetic data. *Geophysical Journal of the Royal Astronomical Society*, *62*(3), 699–718. https://doi.org/10.1111/j.1365-246X.1980.tb02601.x

Knight, K. B., Nomade, S., Renne, P. R., Marzoli, A., Bertrand, H., & Youbi, N. (2004). The Central Atlantic Magmatic Province at the Triassic-Jurassic boundary: Paleomagnetic and 40Ar/39Ar evidence from Morocco for brief, episodic volcanism. *Earth and Planetary Science Letters*, *228*(1-2), 143–160. https://doi.org/10.1016/j.epsl.2004.09.022

Korte, C., Kozur, H. W., Joachimski, M. M., Strauss, H., Veizer, J., & Schwark, L. (2004). Carbon, sulfur, oxygen and strontium isotope records, organic geochemistry and biostratigraphy across the Permian/Triassic boundary in Abadeh, Iran. *International Journal of Earth Sciences*, *93*(4), 565.

Korte, M., Constable, C., Donadini, F., & Holme, R. (2011). Reconstructing the Holocene geomagnetic field. *Earth and Planetary Science Letters*, *312*(3-4), 497–505. https://doi.org/10.1016/j.epsl.2011.10.031

Latypov, R. M. (2002). Phase equilibria constraints on relations of ore-bearing intrusions with flood basalts in the Norilsk region, Russia. *Contributions to Mineralogy and Petrology*, *143*(4), 438–449. https://doi.org/10.1007/s00410-002-0355-8

Lightfoot, P. C., & Keays, R. R. (2005). Siderophile and chalcophile metal variations in flood basalts from the Siberian Trap, Noril'sk Region: Implications for the origin of the Ni–Cu-PGE sulfide ores. *Economic Geology*, *100*(3), 439–462. https://doi.org/10.2113/gsecongeo.100.3.439

Lind, E., Kropotov, S., Czamanske, G., Gromme, S., & Fedorenko, V. (1994). Paleomagnetism of the Siberian flood basalts of the Norilsk area: A constraint on eruption duration. *International Geology Review*, *36*(12), 1139–1150. https://doi.org/10.1080/00206819409465508

Mankinen, E. A., Prévot, M., Grommé, C. S., & Coe, R. S. (1985). The Steens mountain (Oregon) geomagnetic polarity transition: 1. Directional variation, duration of episodes, and rock magnetism. *Journal of Geophysical Research*, *90*, 10,393–10,416. https://doi.org/10.1029/JB090iB12p10393

McElhinny, M. W., & McFadden, P. L. (1997). Palaeosecular variation over the past 5 Myr based on a new generalized database. *Geophysical Journal International*, *131*(2), 240–252. https://doi.org/10.1111/j.1365-246X.1997.tb01219.x
McFadden, P. L., & McElhinny, M. W. (1990). Classification of the reversal test in palaeomagnetism. *Geophysical Journal International*, *103*(3), 725–729. https://doi.org/10.1111/j.1365-246X.1990.tb05683.x
Mikhal'tsov, N., Kazansky, A., Ryabov, V., Shevko, A., Kuprish, O., & Bragin, V. (2012). Paleomagnetism of trap basalts in the northwestern Siberian craton, from core data. *Russian Geology and Geophysics*, *53*(11), 1228–1242. https://doi.org/10.1016/j.rgg.2012.09.009
Moulin, M., Fluteau, F., Courtillot, V., Marsh, J., Delpech, G., Quidelleur, X., & Gérard, M. (2017). Eruptive history of the Karoo lava flows and their impact on early Jurassic environmental change. *Journal of Geophysical Research: Solid Earth*, *122*, 738–772. https://doi.org/10.1002/2016JB013354
Moulin, M., Fluteau, F., Courtillot, V., Marsh, J., Delpech, G., Quidelleur, X., et al. (2011). An attempt to constrain the age, duration, and eruptive history of the Karoo flood basalt: Naude's Nek section (South Africa). *Journal of Geophysical Research*, *116*, B07403. https://doi.org/10.1029/2011JB008210
Naldrett, A. J. (2003). Magmatic sulfide deposits of Nickel-Copper and platinum-metal ores (p. 487). St. Petersburg.
Pavlov, V. E. (2012). Siberian paleomagnetic data and the problem of rigidity of the northern Eurasian continent in the post-Paleozoic. *Izvestiya Physics of the Solid Earth*, *48*(9–10), 721–737. https://doi.org/10.1134/S1069351312080022
Pavlov, V. E., Courtillot, V., Bazhenov, M. L., & Veselovsky, R. V. (2007). Paleomagnetism of the Siberian Traps: New data and a new overall 250 Ma pole for Siberia. *Tectonophysics*, *443*(1-2), 72–92. https://doi.org/10.1016/j.tecto.2007.07.005
Reichow, M. K., Pringle, M. S., Al'Mukhamedov, A. I., Allen, M. B., Andreichev, V. L., Buslov, M. M., et al. (2009). The timing and extent of the eruption of the Siberian Traps Large Igneous Province: Implications for the end-Permian environmental crisis. *Earth and Planetary Science Letters*, *277*(1–2), 9–20. https://doi.org/10.1016/j.epsl.2008.09.030
Renne, P. R., Sprain, C. J., Richards, M. A., Self, S., Vanderkluysen, L., & Pande, K. (2015). State shift in Deccan volcanism at the Cretaceous-Paleogene boundary, possibly induced by impact. *Science*, *350*(6256), 76–78. https://doi.org/10.1126/science.aac7549
Richards, M. A., Alvarez, W., Self, S., Karlstrom, L., Renne, P. R., Manga, M., et al. (2015). Triggering of the largest Deccan eruptions by the Chicxulub impact. *Geological Society of America Bulletin*, *127*(11-12), 1507–1520. https://doi.org/10.1130/B31167.1
Riisager, J., Riisager, P., & Pedersen, A. K. (2003). Paleomagnetism of large igneous provinces: Case-study from West Greenland, North Atlantic igneous province. *Earth and Planetary Science Letters*, *214*(3–4), 409–425. https://doi.org/10.1016/S0012-821X(03)00367-4
Riisager, P., Riisager, J., Abrahamsen, N., & Waagstein, R. (2002). New paleomagnetic pole and magnetostratigraphy of Faroe Islands flood volcanics, North Atlantic igneous province. *Earth and Planetary Science Letters*, *201*(2), 261–276. https://doi.org/10.1016/S0012-821X(02)00720-3
Robock, A. (2000). Volcanic eruptions and climate. *Reviews of Geophysics*, *38*, 191–219. https://doi.org/10.1029/1998RG000054
Saunders, J. E., Pearson, N. J., O'Reilly, S. Y., & Griffin, W. L. (2015). Sulfide metasomatism and the mobility of gold in the lithospheric mantle. *Chemical Geology*, *410*, 149–161. https://doi.org/10.1016/j.chemgeo.2015.06.016
Schmidt, A., Skeffington, R. A., Thordarson, T., Self, S., Forster, P. M., Rap, A., & Carslaw, K. S. (2016). Selective environmental stress from sulphur emitted by continental flood basalt eruptions. *Nature Geoscience*, *9*(1), 77–82. https://doi.org/10.1038/ngeo2588
Schoene, B., Samperton, K. M., Eddy, M. P., Keller, G., Adatte, T., Bowring, S. A., et al. (2015). U-Pb geochronology of the Deccan Traps and relation to the end-Cretaceous mass extinction. *Science*, *347*(6218), 182–184. https://doi.org/10.1126/science.aaa0118
Self, S., Widdowson, M., Thordarson, T., & Jay, A. E. (2006). Volatile fluxes during flood basalt eruptions and potential effects on the global environment: A Deccan perspective. *Earth and Planetary Science Letters*, *248*(1-2), 518–532. https://doi.org/10.1016/j.epsl.2006.05.041
Shcherbakova, V. V., Zhidkov, G. V., Scherbakov, V. P., & Latyshev, A. V. (2013). Estimating the variations in paleointensity from the Siberian Traps of Maymecha-Kotui and Norilsk regions. *Izvestiya Physics of the Solid Earth*, *49*(4), 488–504. https://doi.org/10.1134/S1069351313030142
Svensen, H., Planke, S., Polozov, A. G., Schmidbauer, N., Corfu, F., Podladchikov, Y. Y., & Jamtveit, B. (2009). Siberian gas venting and the end-Permian environmental crisis. *Earth and Planetary Science Letters*, *277*(3-4), 490–500. https://doi.org/10.1016/j.epsl.2008.11.015
Thordarson, T., & Self, S. (2003). Atmospheric and environmental effects of the 1783–1784 Laki eruption: A review and reassessment. *Journal of Geophysical Research*, *108*(D1), 4011. https://doi.org/10.1029/2001JD002042
Torsvik, T. H., van der Voo, R., Meert, J. G., Mosar, J., & Walderhaug, H. J. (2001). Reconstructions of the continents around the North Atlantic at about the 60th parallel. *Earth and Planetary Science Letters*, *187*(1-2), 55–69. https://doi.org/10.1016/S0012-821X(01)00284-9
Valet, J.-P., Fournier, A., Courtillot, V., & Herrero-Bervera, E. (2012). Dynamical similarity of geomagnetic field reversals. *Nature*, *490*(7418), 89–93. https://doi.org/10.1038/nature11491
van der Voo, R., & Torsvik, T. H. (2004). The quality of the European permo-Triassic paleopoles and its impact on Pangea reconstructions. *Geophysical Monograph Series*. https://doi.org/10.1029/145GM03
Vandamme, D. (1994). A new method to determine paleosecular variation. *Physics of the Earth and Planetary Interiors*, *85*(1-2), 131–142. https://doi.org/10.1016/0031-9201(94)90012-4
Vasil'ev, Y. R., Zolotukhin, V. V., Feoktistov, G. D., & Prusskaya, S. N. (2000). Evaluation of the volumes and genesis of Permo-Triassic Trap magmatism of the Siberian platform. *Geologiya i Geofizika*, *41*, 1696–1705.
Watson, G. S. (1956). A test for randomness of directions. *Monthly Notices of the Royal Astronomical Society*, *7*, 160–161. https://doi.org/10.1111/j.1365-246X.1956.tb05561.x
Zijderveld, J. D. A. (1967). Ac demagnetization of rocks: Analysis of results. *Methods in Palaeomagnetism*, *168*(3), 797–810. https://doi.org/10.1016/j.neuroscience.2010.03.066